

A First-Principles Study of the Structure and Dynamics of C_8H_8 , Si_8H_8 , and Ge_8H_8 Molecules

Ç. Kılıç,[†] T. Yildirim,^{*,‡} H. Mehrez,^{†,§} and S. Ciraci[†]

Department of Physics, Bilkent University, Bilkent 06533, Ankara, Turkey, NIST Center for Neutron Research, National Institute of Standards and Technology, Gaithersburg, Maryland 20899, and Department of Physics, McGill University, Quebec, Canada

Received: July 30, 1999; In Final Form: October 29, 1999

We present a first-principles study to elucidate the nature of the bonding, stability, energetics, and dynamics of individual X_8H_8 molecules ($X = C, Si, Ge$). The results obtained from both “local basis” and “pseudopotential” ab initio methods are in good agreement with the experimental data that exists for cubane (C_8H_8). The trends among these molecules are reminiscent of those prevailing in the bulk solids of C, Si, and Ge. High-temperature dynamics and fragmentation of X_8H_8 were studied by the quantum molecular dynamics method which shows that at high temperatures cubane is transformed to the 8-fold ring structure of cyclooctotetraene.

Introduction

Cubane (C_8H_8)^{1,2} is one of the most interesting and unique cage-like structures of carbon-based molecules. As the name “cubane” implies, eight carbon atoms are arranged at the corners of a cube with single hydrogen atoms bonded to each carbon atom along the cube body diagonals. The C–C–C bond angle is therefore 90° rather than the 109.5° normally found in the tetrahedral sp^3 bonding of group IV elements. This bond bending introduces a high strain energy of 6.5 eV in each cubane molecule.³ The cubane structure corresponds to a local minimum on the Born–Oppenheimer energy surface, so that transitions to other structures with lower lying minima would be extremely exothermic. Because of their high heat of formation and high density, the cubane molecule and its derivatives have been considered to be ideal candidates for novel high energetic materials. As a result, the structural and dynamical properties of solid cubane and related materials have recently attracted renewed interest in areas of physics, inorganic chemistry, and organometallics.^{4,7,8} Since silicon and germanium exhibit bulk properties similar to diamond, we may expect Si_8H_8 and Ge_8H_8 to have equally interesting properties. In fact, Si_8H_8 and Ge_8H_8 have yet to be synthesized, though analogies with other chemical groups replacing the hydrogens are known in inorganic chemistry.⁴ For example, the highly symmetrical octahydridosilasesquioxane, $Si_8H_8O_{12}$, has a structure very similar to that of cubane but distorted due to additional oxygen atoms located between Si atoms.^{5,6}

In this paper, we have performed first-principles calculations that elucidate the nature of the bonding, stability, energetics, and dynamics of individual X_8H_8 ($X = C, Si, Ge$) molecules. Furthermore we have carried out constant-temperature quantum molecular dynamics calculations to examine the behavior of these molecules at high temperatures. In this way, we expect to reveal transformations of X_8H_8 to more stable structures. Our

work contributes to the understanding of the design and control of strained molecular systems and corroborates continuing attempts to create new cubane-based materials with novel properties.

Method

Our study includes *first-principles* calculations using both local orbitals and pseudopotential plane wave basis sets. In the first category, we used either standard Gaussian basis sets (e.g., 6-31G*) or others suitable for effective core potentials (i.e. LanL2DZ and CEP-31G*). Using the Gaussian 94 package,^{9,10} we performed (a) self-consistent-field (SCF) calculations with restricted Hartree–Fock (RHF) and perturbation theory to second order (MP2) and (b) density functional theory (DFT) methods within the local spin density approximation (LSDA) with Slater exchange and correlation potential given by Vosko et al.¹¹ Other forms of correlation potential given by Lee et al. (nonlocal, LYP)¹² and Perdew (gradient corrected, P86)¹³ were also used. Further variations on these calculations employed Becke’s three-parameter hybrid form (B3LYP)¹⁴ which also has some nonlocal corrections for correlation. In the second category of calculations, an artificial periodicity, and hence a reciprocal lattice, was introduced by placing the molecule in a large cubic supercell (20 au on a side) that was repeated periodically in three dimensions. The wave functions were expressed as a linear combination of plane waves, $\Psi(\mathbf{k},\mathbf{r}) = \sum_G C_{\mathbf{k}+\mathbf{G}} e^{i(\mathbf{k}+\mathbf{G})\cdot\mathbf{r}}$, in momentum space with a kinetic energy cutoff, $|\mathbf{k} + \mathbf{G}|^2 \leq 50$ Ry. Generalized norm-conserving ionic pseudopotentials¹⁵ with Kleinman–Bylander projectors¹⁸ and a simplified form of generalized gradient approximation given by Perdew et al. (PBE) were used.¹⁹

The optimum size of the supercell and the value of the cutoff energy were determined by our extensive analysis. For example the optimized C–C and C–H bond lengths changed only 0.3% upon increasing the cutoff energy to 60 Ry. The calculated values of these bond lengths are also in very good agreement with those calculated by other techniques.^{16,17}

In the calculations with a Gaussian basis, the molecular X_8H_8 structures were optimized by keeping the O_h symmetry invariant

* Corresponding author. Phone: +1 301 975-6228. Fax: +1 301 921-9847. E-mail: taner@nist.gov. Web: <http://webster.ncnr.nist.gov/staff/taner/>.

[†] Bilkent University.

[‡] NIST.

[§] McGill University.

TABLE 1: Optimized Values of the Bond Lengths d_{XX} and d_{XH} of X_8H_8 Calculated from a LanL2DZ Basis with the B3LYP Exchange-Correlation Potential^a

	X = C	X = Si	X = Ge
d_{XX} (Å)	1.589 (1.558)	2.418 (2.356)	2.556 (2.437)
d_{XH} (Å)	1.089 (1.097)	1.486 (1.485)	1.553 (1.514)
E_F (Ha)	-3.11	-2.09	-1.82
E_g (eV)	8.6	4.8	4.3

^aNumbers shown in parentheses were obtained from quantum molecular dynamics using pseudopotentials with a plane-wave basis. Formation energies E_F and energy gaps E_g of X_8H_8 molecules at the optimized structures are also shown.

t_{1u}		1.428	-1.615	-1.730
t_{2g}		-7.186	-6.408	-6.036
t_{2u}		-7.381	-7.527	-7.394
e_g		-11.540	-8.583	-8.006
t_{1u}		-11.541	-9.969	-9.557
a_{2u}		-12.643	-11.724	-11.852
a_{1g}		-14.387	-11.359	-10.877
t_{2g}		-15.149	-12.851	-13.026
t_{1u}		-19.582	-14.873	-14.884
a_{1g}		-25.498	-17.551	-17.173
		C₈H₈	Si₈H₈	Ge₈H₈

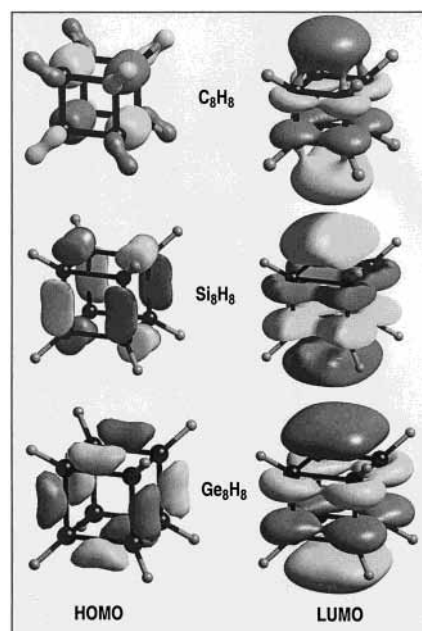
Figure 1. Electronic energy level structure calculated by a LanL2DZ basis with the B3LYP exchange-correlation potential. The uppermost t_{1u} level corresponds to the triply-degenerate LUMO, and below is the t_{2g} HOMO.

while varying the bond lengths, d_{XX} and d_{XH} . The electronic states and the total energy, $E_{X_8H_8}$, were calculated for the optimized structures, and from these the formation energy at $T = 0$ K, $E_F = E_{X_8H_8} - 8(E_X + E_H)$, and the gap, E_g , between LUMO and HOMO were obtained. The vibrational modes were also calculated and their symmetry assignments were determined by analyzing the displacement eigenvectors of the modes. In the pseudopotential plane-wave calculations the structures were optimized using the quantum molecular dynamics method,²⁰ where no constraint on the symmetry was imposed.

Results

Table 1 shows the optimized values of the structural parameters (d_{XX} , d_{XH}), the gap (E_g), and the formation energies (E_F) of the X_8H_8 molecules, which were calculated using a LanL2DZ basis with the B3LYP exchange-correlation potential and pseudopotential plane-wave methods. The corresponding energy levels of the electronic states are summarized in Figure 1.

For C₈H₈, electron diffraction and microwave spectroscopy²¹ yield the values $d_{CC} = 1.571$ Å and $d_{CH} = 1.098$ Å, which are in good agreement with the theoretical calculations. The percentage deviation R_{CC} (R_{CH}) between the calculated and experimental values of d_{CC} (d_{CH}) is about 1% in all cases: $-0.9\% < R_{CC} < 1.1\%$ and $-1.4\% < R_{CH} < 1.6\%$. Note that the bond length d_{XX} increases as the atomic number of X increases. Interestingly, the d_{XX} bond lengths calculated by the pseudopotential plane-wave method are nearly the same as the tetrahedral bond lengths in the corresponding diamond structures. The bond lengths are slightly overestimated by the local basis set calculations. For the energy of formation and the band

**Figure 2.** Isosurfaces of the HOMO and the LUMO for the X_8H_8 molecules. The values of the wave functions on the isosurface of the molecular orbitals are the following: C₈H₈, $|\psi_{HOMO}| = 0.26$ (0.45), $|\psi_{LUMO}| = 0.13$ (0.48); Si₈H₈, $|\psi_{HOMO}| = 0.13$ (0.188), $|\psi_{LUMO}| = 0.075$ (0.152); Ge₈H₈, $|\psi_{HOMO}| = 0.13$ (0.17), $|\psi_{LUMO}| = 0.075$ (0.147). The numbers in parentheses are the maximum amplitude of the wave functions.

gap, we obtained trends similar to those existing for the diamond crystal structure; i.e., E_F and E_g decrease on going from C₈H₈ to Ge₈H₈. On one hand, while E_g is overestimated by the RHF method (predicting $E_g = 15.48$ eV for C₈H₈), it is underestimated by pseudopotential plane-wave calculations within the LDA. This is a well-known limitation in LDA calculations. The energy gap predicted by the DFT calculation with a B3LYP exchange-correlation potential for C₈H₈ results in a reasonable value of $E_g = 8.6$ eV.

In Figure 1, we also note that the width of the valence states (i.e. the energy difference between LUMO and the lowest occupied valence state) for C₈H₈, Si₈H₈, and Ge₈H₈ are 18.3, 11.14, and 11.13 eV, respectively. An interesting result is that the order of the molecular orbitals is almost unchanged with X = C, Si, and Ge (except the consecutive $E_{a_{1g}}$ and $E_{a_{2u}}$ levels are switched in Si₈H₈ and Ge₈H₈). This indicates that most of the orbitals are mainly determined by the O_h symmetry of the molecules. In fact, it was shown²² that in a minimal basis set treatment (i.e. C, 1s2s2p, and H, 1s) several of the molecular orbitals are symmetry-determined. For example, the e_g and t_{2u} orbitals that occur only once in the occupied set (see Figure 1) are symmetry-determined combinations of CC orbitals with no CH admixture.²² Similarly the a_{2u} orbital is derived from a linear combination of CH orbitals with no CC contribution. The high symmetry of the X_8H_8 molecules therefore makes it possible to understand the molecular orbital splitting pattern in terms of interactions between XX and XH orbitals localized mainly on two centers. This is easily seen by inspecting the isosurface of the molecular orbitals. In Figure 2 we plot the wave functions of the HOMO and LUMO. Here we notice that the HOMO of C₈H₈ is quite different from those of Si₈H₈ and Ge₈H₈. However, in all cases, it is mainly a linear combination of two centered XX and XH orbitals. While the HOMO of C₈H₈ has both CC and CH contributions, the HOMO's of Si₈H₈ and Ge₈H₈ are derived mainly by eight XX mixtures. We also note that, in Si₈H₈ and Ge₈H₈, the isosurface of the HOMO is pushed away

E _u	625	215	111	X-X-X bend
T _{2g}	705	227	129	
A _{2u}	1070	344	194	
T _{2g}	837	363	221	X-X stretch
T _{2u}	852	369	217	
T _{1u}	868	373	218	
E _g	930	389	225	
A _{1g}	1015	397	225	
T _{2u}	1083	515	469	X-X-H bend
E _g	1121	552	501	
T _{1g}	1179	529	413	
E _u	1204	545	471	
T _{2g}	1228	617	551	
T _{1u}	1264	654	592	
A _{2u}	3134	2195	2036	X-H stretch
T _{2g}	3148	2200	2041	
T _{1u}	3161	2201	2039	
A _{1g}	3190	2213	2055	
	C₈H₈	Si₈H₈	Ge₈H₈	

Figure 3. Vibrational mode frequencies (in cm⁻¹) and their symmetry assignments calculated with the LanL2DZ basis and the B3LYP exchange-correlation.

from the line connecting the X atoms, a clear indication of weak bonding and highly strained cubane structure. By contrast, the LUMO's of the three X₈H₈ molecules look somewhat similar.

The energies of the vibrational modes and their symmetry assignments, calculated using the LanL2DZ basis with the B3LYP exchange correlation, are shown in Figure 3. A cubic X₈H₈ molecule has 42 internal degrees of freedom and therefore has 42 individual vibrational eigenmodes. As a result of their highly symmetric molecular structure with *O_h* point group symmetry, the vibrational spectrum has only 18 distinct frequencies i.e., 2 × (2A + 5T + 2E). Recently, the vibrational spectrum of C₈H₈ was measured using inelastic neutron scattering methods,²⁴ with the experimental data used to test the transferability of various phenomenological potential models by Yildirim et al.²⁴ The results reported here are in good agreement with the neutron scattering data.

In Figure 3 we show the spectrum of X₈H₈ molecules consisting of four different kind of vibrational modes, assigned to X-X-X bending, X-X stretching, X-X-H bending, and X-H stretching modes; the latter vibrations have the highest energies in the spectrum. We observe that the energy range of these four types of modes and the range of the entire spectrum decreases with increasing atomic number of the element X in the molecule much faster than the expected rate (i.e. 1/√*M* for a harmonic X-X stretch). For example, the ratio of the X-X stretch modes of cubane to that of Si₈H₈ and Ge₈H₈ are about 2.3 and 3.8, respectively. These values are much higher than the expected ratios from mass renormalization of 1.53 and 2.44, respectively. This is a clear indication that the X-X bonding is becoming considerably weaker as the atomic mass increases from C to Ge. Similarly, there is a considerable decrease in the energies of the X-H stretch modes (~42%) of Si₈H₈ and Ge₈H₈ that is solely due to weak bonding between X and H. However unlike the X-X bonding, the X-H bond strengths are very similar in the cases of Si and Ge. We also note that the X-H stretching mode energies are roughly inversely proportional to the corresponding X-H bond lengths.

As discussed above, the results of the calculations with various basis sets and different exchange-correlation potentials for the optimized structure of cubane agree with the experimental data to within a few percent. To compare the accuracy of these

methods in a systematic way, we define an overall error factor $R = \sum_i |(\omega_{\text{calc}}^i - \omega_{\text{exp}}^i)/\omega_{\text{exp}}^i|^2$, where ω_{calc}^i is the calculated (experimental) frequency of the *i*th mode of cubane. Clearly *R* vanishes if the calculation agrees exactly with experiment. The RHF calculation with a 6-31G* basis gives *R* = 0.31, a rather large value that is probably due to the absence of any correlation corrections. Adding second-order corrections with MP2 improves the error factor to *R* = 0.02. The LSDA result is even better with *R* = 0.01 for the 6-31G* basis set with VWN exchange-correlation potential, while the B3LYP potential yields slightly less accurate results with *R* = 0.03. Because our values of *R* is quite small (~0.01), we can say that the accuracy of all of our calculations (excluding the RHF) are acceptable. Moreover, we investigated the effect of the basis set in the case of the B3LYP potential. While the CEP-31G* basis improves the error further (*R* = 0.02), the LanL2DZ yields slightly less accurate results (*R* = 0.04). We conclude that calculations in LanL2DZ with B3LYP exchange-correlation potential are on the same level of accuracy with other first-principles methods.

High-Temperature Quantum Molecular Dynamics

The stabilities of the X₈H₈ molecules were further examined by high-temperature calculations of the total energy.

The optimized structures of X₈H₈ molecules were first obtained by the minimization of the total energy using a dissipative molecular-dynamics algorithm which allows the geometry optimization without any symmetry constraints imposed. The optimized structures were then relaxed at higher temperatures using a Nosé thermostat²⁵ fixed to a desired temperature *T*.

Calculations were performed by using the QMD method with a plane-wave basis set.²⁰ In the structure optimizations, we found the bond lengths came out to be relatively closer to the experimental data when the PBE potential¹⁸ was used in place of the LDA form given by Ceperley and Alder.²⁶ Thus, we used the PBE form in the quantum molecular dynamics simulations.

The structures of the molecules before and after the structural transformation at high temperatures are shown in Figure 4. It appears that while the C₈H₈, Si₈H₈, and Ge₈H₈ molecules are deformed, they are still stable, and the overall features of their cube-based structures are maintained at 1600, 900, and 500 K, respectively. Once the thermostat temperature is increased by 100 K, the cube-based structures of C₈H₈, Si₈H₈, and Ge₈H₈ are modified.

In Figure 4 we first present the snapshots from these modified structures. While the cubane structure is transformed to a stable structure at 1700 K, Si₈H₈ and Ge₈H₈ are not trapped in such a stable structure (at 1000 and 600 K, respectively) within 1 ps relaxation time. Here we did not continue the simulations further to determine the equilibrium high-temperature structures (or the fragmented forms) of Si₈H₈ and Ge₈H₈ since it would take excessive computer time.

We also note that the temperatures at which the structural transformations occur can be lower given a longer relaxation time. Hence, they should be considered as an upper limit to the barrier between the cubane structure and the low-energy less-strained structures shown in Figure 4. Below we concentrate on the relaxed high-temperature structure of C₈H₈ to examine it further.

The structure of C₈H₈ shown at *T* = 1700 K becomes more flattened as *T* increases, and its 8-fold ring structure is eventually destroyed when *T* exceeds 2000 K. This 8-fold ring structure of C₈H₈ has been known since 1911 and is named as cyclo-octetraene.⁴ According to the Hückel (4*n* + 2) rule the ideal

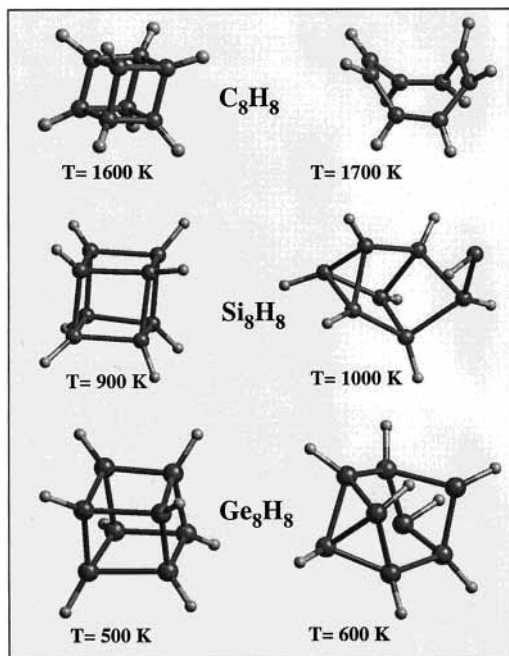


Figure 4. High-temperature structures of the X₈H₈ molecules calculated by quantum molecular dynamics with a plane-wave basis set. The first column shows the structures before transformation, while the second column illustrates how the structure is transformed after a 1 ps relaxation of the original molecule at the given temperature.

planar form of the 8-fold ring that results in C–C–C bond angles of $\phi = 135^\circ$ is nonaromatic, and because the molecular π -orbitals do not form a closed shell, the ring is buckled to shape itself like a tub. Then, each C atom on this buckled ring forms one double bond and one single bond with the neighboring C atoms (all together there are 4 single and 4 double C–C bonds in comparison to the 12 single C–C bonds of cubane) and also one C–H bond with the hydrogen atom.

We further explored the energetics of the 8-fold ring by using a dissipative QMD method at zero temperature. As described in the inset to Figure 5, the buckling of the 8-fold ring is characterized by the C–C–C bond angle ϕ and three different bonds, i.e., d_{CC}^l , d_{CC}^s , and d_{CH} . In the course of optimization the structure returned to the cubane structure when $\phi \leq 105^\circ$.

As the bond angle varies in the range $115^\circ < \phi < 135^\circ$, the 8-fold ring structure traced the parabola; each time it was trapped in a local minimum for the values of the bond angles indicated by the diamonds in Figure 4. The bond lengths d_{CC}^l , d_{CC}^s , and d_{CH} remain practically unaltered. Since $\Delta E(\phi)$ at the minimum ϕ_0 is negative, the 8-fold buckled ring with $\phi_0 \sim 127^\circ$, i.e., cyclooctatetraene, corresponds to a local minimum of the Born–Oppenheimer surface and is found to be more stable than cubane with $|\Delta E| = 2.66$ eV. Calculations of ϕ_0 (via structure optimization) and ΔE using the 6-31G* Gaussian basis set provide agreement with the pseudopotential plane wave calculations. RHF and DFT using the B3LYP potential yield respectively 3.5 and 3.3 eV for ΔE and 127.3° and 127.7° for ϕ_0 . However, a DFT calculation using Slater exchange and P86 correlations yields a rather small energy ($\Delta E \sim 1.0$ eV) and $\phi_0 = 126^\circ$. Recently, seven different structures with the chemical formula C₈H₈ were located on the potential energy surface of cyclooctatetraene.²⁷ The relationship between cubane and cyclooctatetraene is established in the present work. This finding could be useful in designing new routes to synthesize cubane based materials.

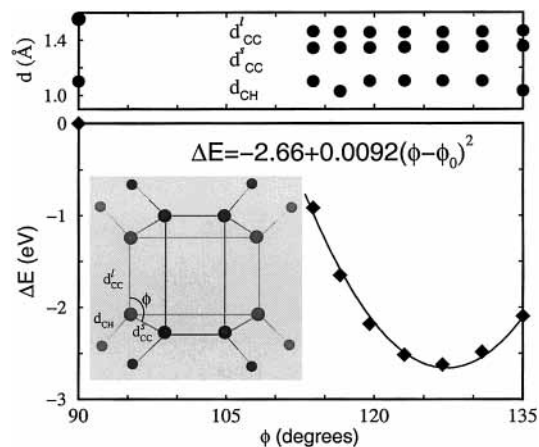


Figure 5. Top: Variations of the bond lengths (long C–C bond d_{CC}^l , short C–C bond d_{CC}^s , and C–H bond d_{CH}) as a function of the angle ϕ . Bottom: Variation of the total energy relative to cubane ΔE with the angle ϕ . Relevant structural parameters are shown in the inset.

Conclusion

In summary, we have investigated various aspects of the structural, electronic, and dynamical and high-temperature behavior of individual X₈H₈ molecules. Calculations for cubane are in good agreement with the available experimental data. Our results indicate that as the atomic number of X increases, the gap between LUMO and HOMO, formation energy, width of the valence electronic states, and frequencies of the vibrational modes all decrease, while their volume and bond lengths increase. The temperature-dependent quantum molecular dynamics calculations predict that the cubane molecule transforms to the more stable cyclooctotetraene molecule at a temperature $1600 \text{ K} < T < 1700 \text{ K}$. Si₈H₈ and Ge₈H₈ are also metastable at two local minima of the Born–Oppenheimer surface, which are separated by small energy barriers from other more stable structures.

Acknowledgment. We thank U. Salzner for stimulating discussions. The authors acknowledge partial supports from the National Science Foundation under Grant No. INT97-31014 and TÜBİTAK under Grant No. TBAG-1668(197 T 116). The quantum molecular-dynamics calculations were performed by using the code JEEP provided by F. Gygi.

References and Notes

- (1) Eaton, P. E.; Cole, T. W., Jr. *J. Am. Chem. Soc.* **1964**, *86*, 962.
- (2) Eaton, P. E. *Angew. Chem.* **1992**, *31*, 1421.
- (3) Kybett, B. D.; Carroll, S.; Natollis, P.; Bonnell, D. W.; Margrave, J. L.; Franklin, J. L. *J. Am. Chem. Soc.* **1966**, *88*, 626. Borman, S. *Chem. Sci. Eng. News* **1994**, *72*, 34.
- (4) Cotton, F. A. *Advanced Inorganic Chemistry*; Wiley: New York, 1988.
- (5) Bartsch, M.; Bornhauser, P.; Calzaferri, G.; Imhof, R. *Vib. Spectrosc.* **1995**, *8*, 305.
- (6) Marcolli, C.; Laine, P.; Buhler, R.; Calzaferri, G.; Tomkinson, J. *J. Phys. Chem. B* **1999**, *101*, 1171.
- (7) Liu, W.; Dolg, M.; Fulde, P. *J. Chem. Phys.* **1997**, *107*, 3854.
- (8) Yildirim, T.; Gehring, P. M.; Neumann, D. A.; Eaton, P. E.; Emrick, T. *Phys. Rev. Lett.* **1997**, *78*, 4938; **1998**, *36*, 809; *Phys. Rev. B* **1999**, *60*, 314.
- (9) *Gaussian 94*; Gaussian, Inc.: Pittsburgh, PA, 1995.
- (10) Identification of commercial products does not imply recommendation or endorsement by the National Institute of Standards and Technology.
- (11) Vosko, S. H.; Wilk, L.; Nusair, M. *Can. J. Phys.* **1980**, *58*, 1200.
- (12) Lee, C.; Yang, W.; Parr, R. G. *Phys. Rev. B* **1988**, *37*, 785.
- (13) Perdew, J. P. *Phys. Rev. B* **1986**, *33*, 8822.
- (14) Becke, A. D. *J. Chem. Phys.* **1993**, *98*, 5648.
- (15) Hamann, D. R. *Phys. Rev. B* **1989**, *40*, 2980.
- (16) Yildirim, T.; et al. *Phys. Rev. B*, in press.

- (17) Richardson, S. L.; Martins, J. L. *Phys. Rev. B* **1998**, *58*, 15307.
- (18) Kleinman, L.; Bylander, D. M. *Phys. Rev. Lett.* **1982**, *48*, 1425.
- (19) Perdew, J. P.; Burke, K.; Ernzerhof, M. *Phys. Rev. Lett.* **1982**, *77*, 3865.
- (20) Car, R.; Parrinello, M. *Phys. Rev. Lett.* **1985**, *55*, 2471.
- (21) Hedberg, L.; Hedberg, K.; Eaton, P. E.; Nodari, N.; Robiette, A. G. *J. Am. Chem. Soc.* **1991**, *113*, 1514.
- (22) Schulman, J. M.; Fischer, C. R.; Solomon, P.; Venanzi, T. J. *J. Am. Chem. Soc.* **1978**, *100*, 2949.
- (23) Cole, T. W., Jr.; Perkins, J.; Putnam, S.; Pakes, P. W.; Strauss, H. L. *J. Am. Chem. Soc.* **1981**, *85*, 2185.
- (24) Yildirim, T.; Kılıç, Ç.; Ciraci, S.; Gehring, P. M.; Neumann, D. A.; Eaton, P. E.; Emrick, T. *Chem. Phys. Lett.* **1999**, *309*, 234–240.
- (25) Nosé, S. *J. Chem. Phys.* **1984**, *81*, 511.
- (26) Ceperley, D. M.; Alder, B. J. *Phys. Rev. Lett.* **1980**, *45*, 556.
- (27) Andrés, J. L.; Castano, O.; Morreale, A.; Palmeiro, R.; Gomperts, R. *J. Chem. Phys.* **1998**, *108*, 203.